Progress In Electromagnetics Research Letters, Vol. 110, 63–71, 2023

Isolation and Gain Improvement of Multiple Input Multiple Output Antenna Using Frequency Selective Surfaces

Anett Antony* **and Bidisha Dasgupta**

Abstract—This letter addresses a new approach to improve the gain and isolation of a multiple input multiple output (MIMO) antenna. A C-shaped printed antenna with both ends terminated by a small rectangular section is designed as the basic antenna element for a 2 element MIMO antenna of size $0.8\lambda \times 0.67\lambda \times 0.04\lambda$ (λ, corresponding to the lowest operating frequency) which operates over the X band with the peak gain of 3 dBi. By introducing a double layered frequency selective surface (FSS) of unit cell dimension $0.2\lambda \times 0.2\lambda \times 0.0375\lambda$ between the two antenna elements as an isolation wall and additionally by placing a 5×3 array of FSS geometry as a reflector below the antenna, the isolation and gain of the two element MIMO antenna are improved by 37 dB and 3 dBi, respectively. The proposed FSS loaded MIMO antenna provides very high isolation about -51 dB (measured) and a very low envelope correlation coefficient (ECC) of 0.000177282 (simulated) using far field approach and 0.000000033414 (calculated measured) using scattering (S) parameter approach. Further, MIMO parameters like diversity gain (DG), total active reflection coefficient (TARC), mean effective gain (MEG), and channel capacity loss (CCL) have been evaluated. The radiation pattern is unidirectional in nature with a peak gain about 6 dBi. The letter also presents detailed design guidelines for the proposed FSS loaded MIMO antenna along with their verifications for Ku and K bands. The proposed structure can also be scaled up to a 4 element MIMO antenna.

1. INTRODUCTION

Multiple input multiple output (MIMO) technology is one of the leading techniques used in the fourth and fifth generation communication systems, which helps in increasing the channel capacity and reliability without burdening the available spectrum. Here multiple antennas are used which helps in providing spatial multiplexing or spatial diversity [1]. The multiple antennas are kept close to each other due to space constraints, but this can lead to the coupling between the antenna elements which can degrade the performance of the MIMO system. So, the basic requirements as well as the challenges of MIMO antennas are to maintain high isolation and low envelope correlation coefficient (ECC) between closely spaced antenna elements along with obtaining a directional radiation pattern with suitable gain. Some decoupling methods adopted in the past literature are using neutralization lines [1], defected ground structures [1], parasitic elements [1], split ring resonator structures [2], electromagnetic band gap structures [2], metamaterials/frequency selective surface (FSS) [3–6], metallic wall [7], partially reflecting surface (PRS) [1], etc. The metamaterial/FSS provides very good performance in terms of ECC and diversity gain (DG) [2]. Das et al. [1] designed a PRS which tilted the radiation pattern of antenna elements in opposite directions and hence helped in isolating the far field patterns. Si et al. [3] designed a metamaterial with positive permittivity and negative permeability, and it was placed on the top of a MIMO antenna for isolation improvement. In [5–7], metamaterial wall, FSS wall, and

Received 15 March 2023, Accepted 15 April 2023, Scheduled 26 April 2023
* Corresponding author: Anett Antony (anett.anthony@iiitg.ac.in).
The authors are with the Department of Electronics and Communication Engineering, Indian Institute of Information Technology Guwahati, India.

metal wall respectively were designed and placed between antenna elements for isolation improvement. Although the above methods provided isolation improvement, their operating bandwidth was less than or equal to 2 GHz. In the past, a few works had been reported on the decoupling of free space radiation of MIMO antenna using periodic structures like metamaterial/metasurface/FSS, etc. A comprehensive study of some of such past works is discussed in a comprehensive manner in Section 7.

FSS is a category under planar metamaterials and is quite popular due to its ease of fabrication. It is a subwavelength periodic arrangement of different shapes which act as spatial filters [8]. It is used in a wide range of applications like [9] as a reflector, absorber, polarizer, for radar cross section reduction (RCS), etc. As per the past study, a multilayer FSS offers better bandwidth than a single layer FSS [9].

The past literature reveals the fact that the FSS is a potential candidate for MIMO antenna [2], but it was explored very little. Considering these facts, in this paper the authors present a new approach to improve the gain and isolation of the MIMO antenna, which operates over the whole X band. The same FSS structure has been placed between as well as below the antenna elements in a MIMO antenna for improving such parameters significantly. Additionally, the authors have developed and presented a design guideline which can be used to design the MIMO antennas for Ku and K bands. The proposed structure is further extended to design a 4 element MIMO antenna. The methodology adopted is briefly discussed in Section 2. The development of the standalone antenna and FSS geometries are discussed in Section 3. The performance of the MIMO antenna when it is loaded with an FSS wall and FSS at the back is discussed in Section 4, and the measured results are provided in Section 5. The design guidelines to design both the antenna and FSS geometries at different bands are provided in Section 6, and Section 7 concludes the paper.

2. BRIEF METHODOLOGY

In order to use an FSS as a reflector for an antenna, it is required that the transmission bandwidth (S_{12}, $S_{21} \leq -10\,\text{dB}$, S_{11}, $S_{22} \sim 0\,\text{dB}$) of the FSS needs to be compatible with the impedance bandwidth of the antenna element (i.e., $S_{ii} \leq -10\,\text{dB}$, VSWR < 2, i = number of antenna port). In the proposed work, the same FSS structure has been placed between as well as below the antenna elements in a MIMO antenna. In this case, the FSS which is placed between the antenna elements improves the isolation, and the FSS placed below the antenna surface at a suitable distance mainly improves the directional gain of the antenna in forward direction due to the constructive interference between the reflected backward radiation and forward radiation of the antenna by utilizing the total radiated power. To implement this idea, a two element MIMO antenna is designed along with an FSS geometry for X band. Both antenna and FSS geometries are new in shape. By introducing a double layered FSS between the two antenna elements, the isolation between the two elements of the MIMO antenna is primarily improved, and by placing a 5×3 array of the same FSS beneath the antenna, the directional gain of the proposed MIMO antenna is improved. The perspective view of the proposed structure along with the top and bottom views of the antenna and the FSS geometries is provided in Fig. 1. The simulation study and parametric optimization have been done by using HFSS [10].

3. ANTENNA AND FSS GEOMETRY

3.1. MIMO Antenna Geometry

The proposed MIMO antenna contains two antenna elements with partial ground plane, as shown in Figs. 1(b) and 1(c), and a microstrip line is used as feed. The basic antenna element is originated from a circular patch (CP) shaped structure as shown in Fig. 2(a)(i) and is developed at center frequency of X band by using Equation (2.30) in [11] for TM_{21} mode. The effective radius (a_e) is calculated by using Equation (2.31) in [11]. In order to minimize the ohmic losses and to improve the impedance matching, the CP is modified chronologically as shown in Fig. 2(a)(i)–(iv), i.e., from CP to a semi-circular patch (SCP), then to C-shaped patch, and finally, two small rectangular sections are introduced at both ends of the C-shaped patch, as shown in Fig. 2(a)(iv). Improvement in impedance matching is observed at every stage of the chronological development of the antenna structure, as shown in Fig. 2(a). The proposed antenna operates from 8.1 to 12.77 GHz ($S_{11} \leq -10\,\text{dB}$, VSWR < 2) with S_{11} minima at

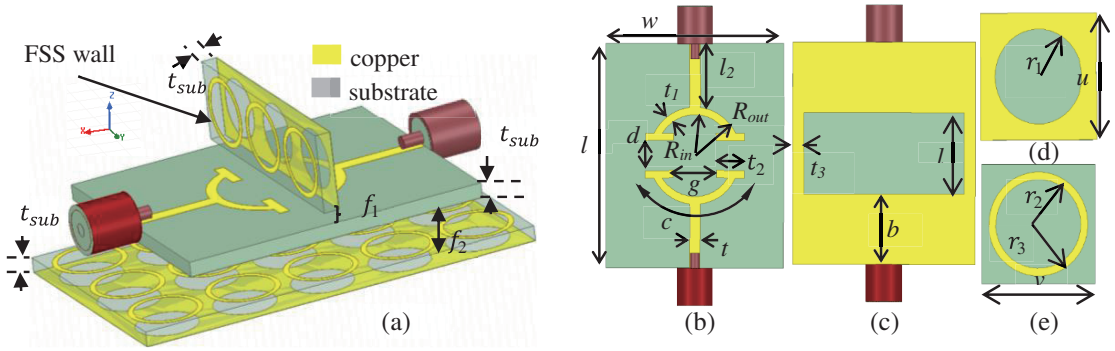

Figure 1. (a) Perspective view of the proposed MIMO antenna loaded with FSS, (b) top view, (c) bottom view of the proposed MIMO antenna, (d) bottom view and (e) top view of the proposed FSS unit cell.

9.6 GHz and 11.8 GHz. Two proposed antenna structures are placed face to face to get a two element MIMO antenna, and the interelement space between the antenna elements is kept about 4 mm ($0.13\lambda_o$ corresponding to 10.4 GHz, which is the center frequency of the operating band). The dimensions are provided in Table 1. An FR 4 epoxy substrate of thickness (t_{sub}) 1.5 mm with dielectric constant 4.4 and loss tangent 0.002 is used for antenna designing.

Table 1. Dimensions of the proposed antenna and FSS geometry (Dimensions are in mm).

$f_2 = 4.5$	$f_1 = 1$	$t_{sub} = 1.5$	$l = 11$	$l_1 = 30$	$l_2 = 8.5$	$r_1 = 3$	$t = 1.5$	$c = 12.56$	$r_3 = 3$	$t_3 = 1.5$
$u = 8$	$v = 8$	$w = 25$	$r_2 = 2.5$	$d = 4$	$R_{out} = 6.5$	$t_1 = 1,$	$t_2 = 4,$	$R_{in} = 5.5$	$g = 6$	$b = 9.5$

3.2. FSS Geometry

In the present work, it is targeted to design FSS as a reflector which is compatible with the proposed MIMO antenna operating in the X band. In stage-1, a single layer FSS geometry of circular metallic loop is designed on an FR-4 epoxy substrate of thickness (t_{sub}) 1.5 mm. After that in stage-2, an aperture circular loop on conducting screen is introduced on the other side of the substrate, and finally the proposed structure as shown in Figs. 1(d) and 1(e) is obtained, where one side is a circular aperture on a conducting screen (Fig. 1(d)), and other side is a conducting circular loop (Fig. 1(e)). The dimensions of the proposed FSS geometry are provided in Table 1. The single FSS layer alone could not cover the operating band of the antenna, so double layered FSS was designed. The proposed FSS operates as a reflector from 7.5 to 14.6 GHz ($S_{12} \leq -10$ dB, $S_{11} \sim 0$ dB), as shown in Fig. 2(b). The reflection phase of the proposed structure is also found to be approximately linear, as shown in Fig. 2(b). The proposed FSS geometry is examined for angular and polarization stabilities, and it is found to be stable for both the cases as shown in Fig. 2(c) and Fig. 2(d), respectively.

4. MIMO ANTENNA LOADED WITH FSS

A 3 element FSS wall is first introduced in between the two element MIMO antenna as shown in Fig. 1(a). This reflector wall helps in decoupling the field interaction between the antenna elements as shown in Fig. 3(a)(ii), and the isolation obtained is near −20 dB over the operating band. The peak gain of the structure is about 3 dBi. Afterwards, a 5×3 array of FSS geometry is placed beneath the antenna which changes the radiation pattern from bidirectional to unidirectional (Fig. 3(a)(iii)) and also increases the peak gain to about 6 dBi. There is also a significant improvement in the isolation level (simulated) from −13 dB to −55 dB, at 10 GHz as shown in Fig. 3(b). A detailed parametric analysis

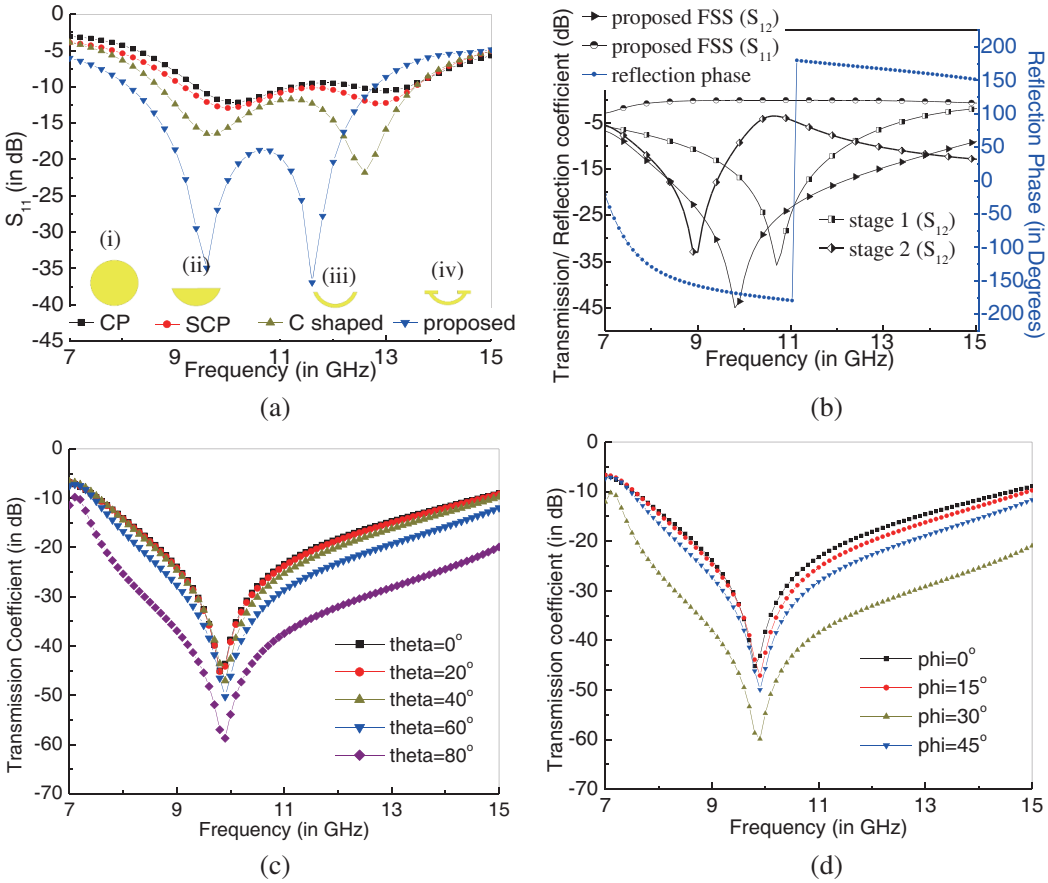

Figure 2. (a) S_{11} characteristics for various stages of the antenna structure (i) circular patch (CP), (ii) semi-circular patch (SCP), (iii) C shaped patch and (iv) proposed patch, (b) transmission characteristics of the various stages of FSS with reflection characteristics of the proposed FSS structure, (c) transmission characteristics under oblique incidence, and (d) transmission characteristics under different polarization angles.

has been carried out to optimize the distances (f_1, f_2) and also the sizes of the FSS wall between and below the antenna elements. The results are shown in Figs. 3(c)–3(f) which reveals the fact that a 3 element FSS wall at $f_1 = 1$ mm and a 5×3 array of FSS geometry below the MIMO antenna at $f_2 = 4.5$ mm offers the best result.

5. MEASURED RESULTS

The fabricated prototype is shown in Fig. 3(g). The measurement of the S parameters has been done using an in-house Vector Network Analyzer (VNA) (make: Anritsu, model number: MS2028C VNA Master) and the radiation characteristics using microwave signal generator (make: Keysight Technologies, model no: N5173B), standard gain pyramidal X band horn antenna, turn table, and USB power sensor (make: Anritsu, model no: MA24118A). The frequencies corresponding to S_{11}/S_{12} minima are nearly similar in simulated and measured characteristics, as shown in Fig. 3(b). The fabrication tolerances like characteristic of material used, soldering material, and imperfections in some connectors (like commercial probe, SMA connectors) cause some deviations in the S parameter characteristics of the prototype at some frequencies from the simulated ones.

The simulated and measured radiation patterns for both MIMO antenna and MIMO antenna backed with FSS and FSS wall are shown in Fig. 4 for both $\Phi = 0°$ and $\Phi = 90°$ planes. The simulated and

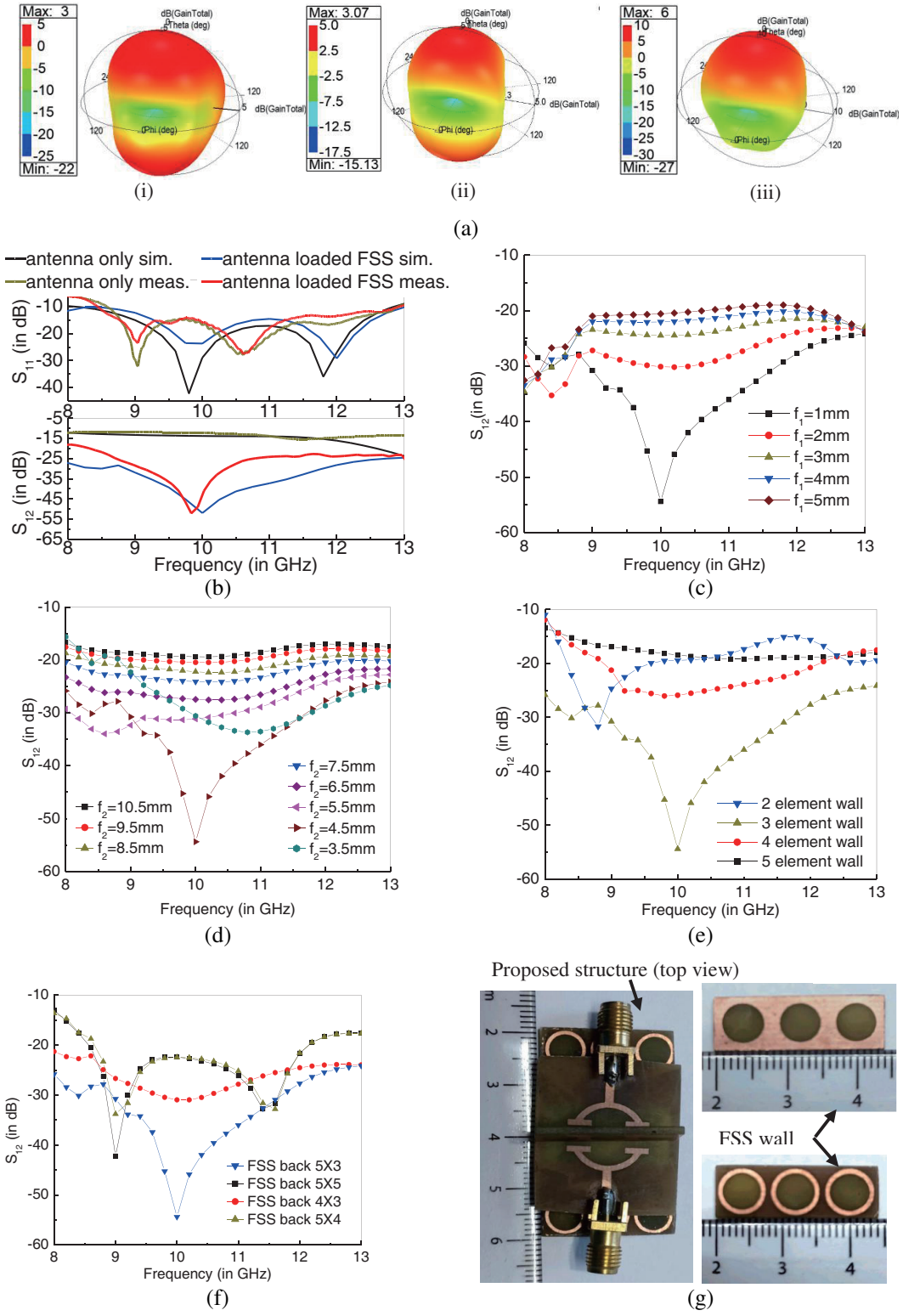

Figure 3. (a) The simulated far field radiation pattern at 10 GHz for (i) MIMO antenna only, (ii) MIMO antenna with FSS wall and (iii) MIMO antenna backed with FSS and FSS wall, (b) measured and simulated S parameters of antenna and antenna loaded with FSS, parametric analysis for (c) f_1, (d) f_2, (e) FSS wall, (f) FSS in the back and (g) fabricated antenna and FSS geometries.

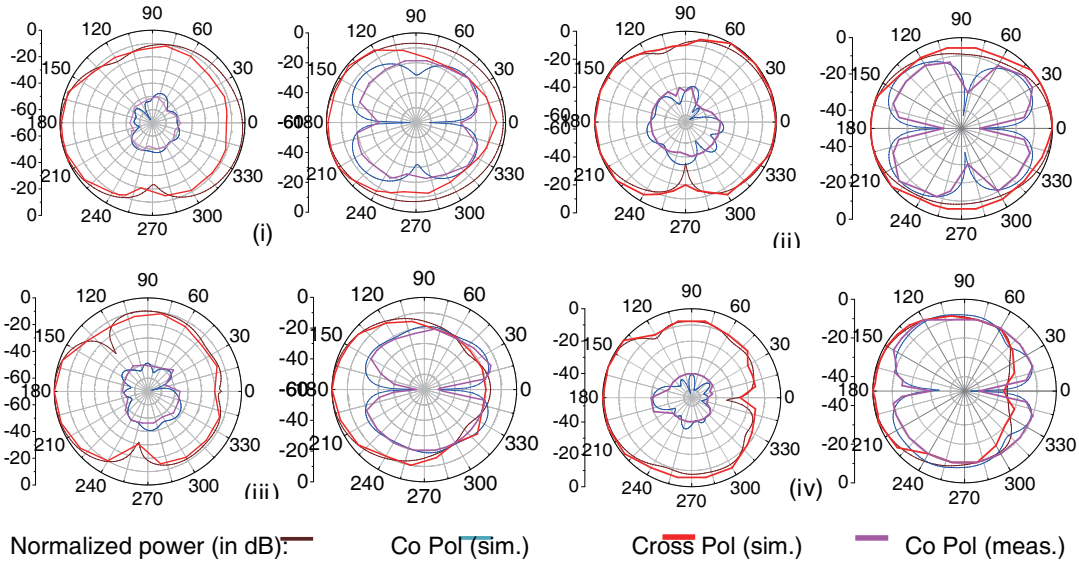

Figure 4. The normalized power pattern at (i) 10 GHz, (ii) 12 GHz for MIMO antenna and at (iii) 10 GHz, (iv) 12 GHz for MIMO antenna backed with FSS and FSS wall.

measured peak realized gains are plotted in Fig. 5(a). The ECC due to far field is given as [6]

$$ECC_{\text{far field}} = \frac{\left| \iint\limits_{4\pi} \left[\vec{F}_1(\theta,\phi) * \vec{F}_2(\theta,\phi) \right] \mathrm{d}\Omega \right|}{\sqrt{\iint\limits_{4\pi} \left| \vec{F}_1(\theta,\phi) \right|^2 \mathrm{d}\Omega \iint\limits_{4\pi} \left| \vec{F}_2(\theta,\phi) \right|^2 \mathrm{d}\Omega}} \tag{1}$$

where $F_i(\theta\phi)$ is the radiated field when only the ith element is excited. The ECC by using the S-parameters is computed by using the following formula [6]

$$ECC_{S\text{ parameter}} = \frac{\left| S_{ii}^* S_{ij} + S_{ji}^* S_{jj} \right|^2}{(1 - |S_{ii}|^2 - |S_{ij}|^2)(1 - |S_{ji}|^2 - |S_{jj}|^2)} \tag{2}$$

The simulated ECC (based on far field) is less than 0.08, and the calculated measured ECC (based on S parameters, which is calculated using Equation (2)) is less than 0.00097, both of which are quite low and are plotted in Fig. 5(a).

Diversity gain (DG) is a parameter calculated using ECC and given as [6]

$$DG = 10\sqrt{1 - (ECC)^2} \tag{3}$$

The simulated and calculated measured DGs of the proposed MIMO antenna using S parameter approach are approximately near 10 dB, and the simulated DG using the far field approach lies near 9.98 dB and is shown in Fig. 5(b). So the proposed structure provides good diversity performance. The total active reflection coefficient (TARC) is another parameter considered for MIMO antennas [6]. The value of TARC should not exceed 0 dB. For the proposed MIMO antenna, the simulated and calculated measured TARCs lie below −4 dB with minimum TARC lying near −14 dB and are shown in Fig. 5(c). The channel capacity loss (CCL) is considered as a significant parameter in channel performance analysis of MIMO antennas [12]. Ideally, the value of CCL is required to be zero. For the proposed antenna the simulated minimum CCL is 0.014095 bps/Hz. The simulated CCL lies below 0.3 bps/Hz over the whole band, and the calculated measured CCL lies near 0.5 bps/Hz over the whole band. Both the simulated and calculated measured mean effective gains (MEGs) are acceptable and lie below −3 dB

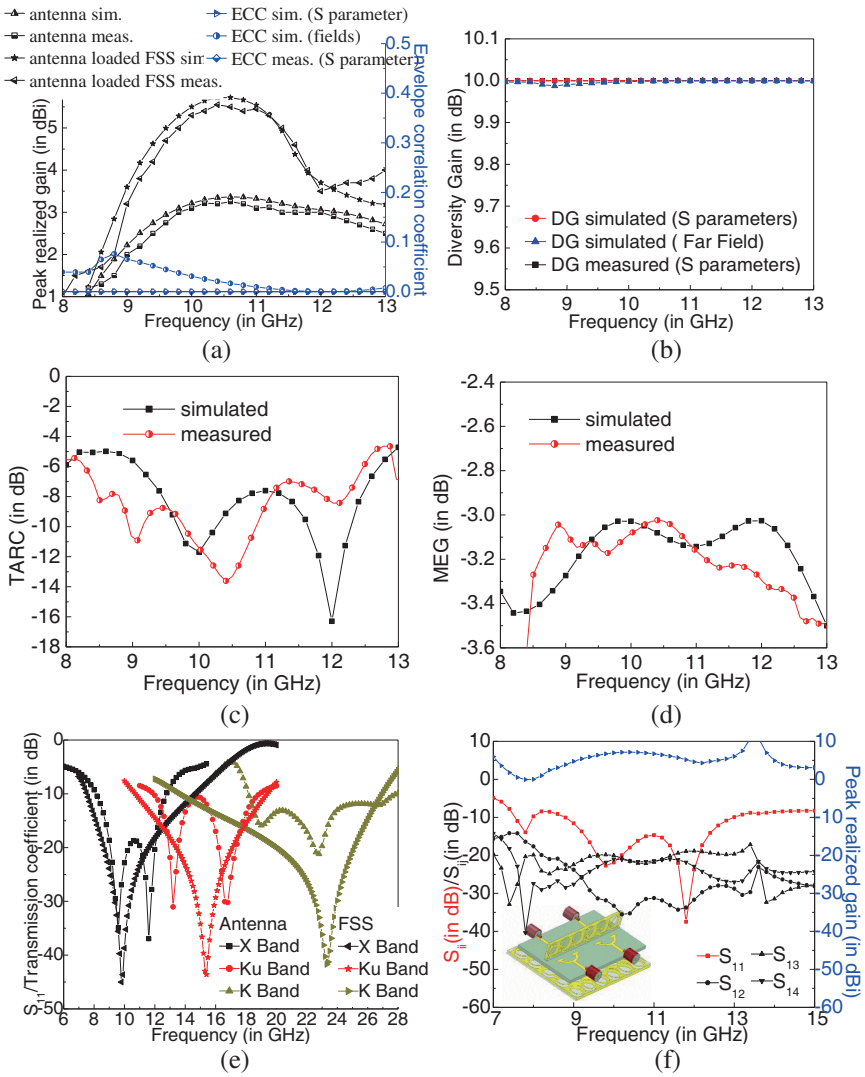

Figure 5. Simulated and measured (a) peak realized gain and ECC, (b) DG, (c) TARC and (d) MEG of the proposed MIMO antenna loaded with FSS, (e) design verification for antenna and FSS, (f) S parameter and peak realized gain for four element MIMO with four element MIMO antenna shown in inset.

over the whole band, shown in Fig. 5(d). The radiation efficiency of the proposed antenna lies between 78 and 88 percent.

6. DESIGN PROCEDURE AND VERIFICATION

This section describes the procedure for designing both the antenna and the FSS at different frequency bands. Here, f_u is the upper operating frequency, f_l the lower operating frequency, and f_c the center frequency.

6.1. Antenna

1) Frequency of operation: The ratio bandwidth (RB) is defined as $f_u \approx 1.5 f_l$.
2) Dimension of ground plane: λ_c is the wavelength corresponding to f_c, then $b \approx \lambda_c/3$, $t_3 \approx \lambda_c/20$ and $0.8\lambda_c \leq w \leq 1.2\lambda_c$.

3) Dimension of the CP: The CP for radius $(R_{out} + R_{in})/2$ is calculated for the center frequencies of the respective bands using Equation (2.31) in [11]. Circumference of the sectoral portion is $0.4\lambda_c \leq c \leq 0.6\lambda_c$.
4) The ratio of $g/t_2 \approx \lambda_c/20$.

6.2. FSS

1) Frequency of operation: The ratio bandwidth (RB) is defined as $f_u \approx 1.5 f_l$.
2) The average radius $r = (r_2 + r_3)/2$ of the circular loop on the top side of the FSS structure is $0.1\lambda_c \leq r \leq 0.12\lambda_c$.
3) The length of the unit cell u is $0.3\lambda_c \leq u \leq 0.33\lambda_c$.

The dimensions of the parameters of both antenna and FSS designed using the design guidelines are shown in Table 2, and the design verification is shown in Fig. 5(e) for both antenna and FSS. All the dimensions can be further optimized to achieve better result.

Table 2. Design parameters of antenna and FSS.

Design frequency (in GHz): Antenna	RB	Ground Plane†			Patch†			Design frequency (in GHz): FSS	RB	FSS†	
		b	t_3	w	a	c	g/t_2			r	u
Proposed: 8.1–12.7	1.56	9.5	1.5	25	6	12.56	1.5	Proposed: 7.5–14.6	1.94	3	8
Design 1 12–18.7	1.58	7	1.25	20	5	9.82	1.25	Design 1 10.8–19.3	1.78	2.5	6.5
Design 2 18–27.8	1.53	5	1	16	4	8.68	1	Design 2 13.7–26.9	1.93	1.5	4.5

†The dimension of all the parameters is in mm

Table 3. Comparison of the proposed structure with some existing works.

Ref. No., year	Method adopted with position	Antenna dimension $\mathbf{L} \times \mathbf{W} \times \mathbf{T}^{*\#}$; shape**; No. of elements	Isolation; Isolation improvement (in dB);	ECC	Operating frequency (in GHz)	Edge-Edge/ Center-Center spacing (in λ_o/mm)	Gain; Gain improvement (in dBi)
[1], 2019	Partially reflecting surface on top	$2\lambda \times 1.75\lambda \times 0.03\lambda$; CDRA height: 7.8,6.7,6; 6	−23; 10–20	≤ 0.12 (Field)	5.15–5.35, 5.4–5.65, 5.7–5.9	$0.31\lambda_o$, $0.33\lambda_o$, $0.35\lambda_o/18$	$\approx 8; 2$
[3], 2019	Metamaterial on top	$0.6\lambda \times 0.36\lambda \times 0.042\lambda$; rectangular patch; 2	−29; 23	Not given	4.2–5.25	$0.017\lambda_o/1$	6.59; 3.2
[5], 2020	Metamaterial absorber wall	Not given; rectangular patch; 2	−43.71; 21.6	0.00043 (S parameter)	5.5 WiMAX	$0.5\lambda_o/30$	7.74; 0.21
[7], 2021	Metal wall with FSS in the top	$0.74\lambda \times 0.74\lambda \times 0.03\lambda$; circular patch; 2	−59.5; 20	≤ 0.004 (Field) 0.0002 (S parameter)	4–5.3	8	4, 0.8
[6], 2022	FSS wall with AMC in the back	Not given; bow tie antenna; 2	≈ -30; ≈ 12	≤ 0.05 (S parameter)	2.95–4.95	$0.18\lambda_o$	8; 0.7
Proposed work	Same FSS as wall and in the back	$0.8\lambda \times 0.67\lambda \times 0.04\lambda$; C shaped with rectangular arms; 2	−51 (measured); 40	0.000177282 (Field) 0.000000033414 (S parameter)	8.4–13	$0.13\lambda_o/4$	5.6; 2.6

*L =length, W =width and T =thickness, #λ corresponding to the lowest operating frequency
**The height of the FSS/PEC/AMC/PRS has not been considered
AMC: Artificial magnetic conductor, S parameter: scattering parameter

7. CONCLUSION

The present study reveals the fact that by designing a suitable FSS geometry as a reflector which is compatible with the MIMO antenna, and by placing it properly between and below the MIMO antenna elements, it is possible to improve the directional gain and isolation of MIMO antenna. The improvement of such parameters of the proposed 2 element X-band MIMO antenna is better than the past work and is tabulated in Table 3. The proposed structure can also be scaled up to 4 element MIMO antenna as shown in the inset of Fig. 5(f) while maintaining the isolation, bandwidth, and peak realized gain as shown in Fig. 5(f). The design guidelines of the proposed MIMO antenna can also be used to develop a MIMO antenna for Ku and K band applications.

ACKNOWLEDGMENT

The authors are thankful to Mr. Kishore Kumar Das for providing the needful assistance in performing the experiments. The first author acknowledges the financial support of UGC India through a fellowship (NTA Ref. No.: 200510980526 dated10/12/2020).

REFERENCES

1. Das, G., A. Sharma, R. K. Gangwar, and M. S. Sharawi, "Performance improvement of multi-band MIMO dielectric resonator antenna system with a partially reflecting surface," *IEEE Anten. Wire. Propag. Lett.*, Vol. 18, No. 10, 2105–2109, Oct. 2019.
2. Kumar, S., A. S. Dixit, R. R. Malekar, H. D. Raut, and L. K. Shevada, "Fifth generation antennas: A comprehensive review of design and performance enhancement techniques," *IEEE Access*, Vol. 8, 163568–163593, Sept. 2020.
3. Si, L., H. Jiang, X. Lv, and J. Ding, "Broadband extremely close-spaced 5G MIMO antenna with mutual coupling reduction using metamaterial-inspired superstrate," *Optics Exp.*, Vol. 27, No. 3, 3472–3482, Feb. 2019.
4. Karimian, R., A. Kesavan, M. Nedil, and T. A. Denidni, "Low-mutual-coupling 60-GHz MIMO antenna system with frequency selective surface wall," *IEEE Anten. Wire. Propag. Lett.*, Vol. 16, 373–376, Jun. 2017.
5. Garg, P. and P. Jain, "Isolation improvement of MIMO antenna using a novel flower shaped metamaterial absorber at 5.5 GHz WiMAX band," *IEEE Trans. on Circuits Systems II: Express Briefs*, Vol. 67, No. 4, 675–679, Apr. 2020.
6. Anudeep, B., K. Krishnamoorthy, and P. H. Rao, "Low-profile, wideband dual-polarized 1×2 MIMO antenna with FSS decoupling technique," *Int. J. Microw. Wire. Techno.*, Vol. 14, No. 5, 634–640, Jun. 2022.
7. Mondal, R., P. S. Reddy, D. C. Sarkar, and P. P. Sarkar, "Investigation on MIMO antenna for very low ECC and isolation characteristics using FSS and metal-wall," *AEU-Int. J. Electron. Comm.*, Vol. 135, 1–9, Jun. 2021.
8. Munk, B. A., *Frequency Selective Surfaces — Theory and Design*, John Wiley & Sons, New York, 2000.
9. Bhattacharya, A., B. Dasgupta, and R. Jyoti, "A simple frequency selective surface structure for performance improvement of ultra-wideband antenna in frequency and time domains," *Inter. J. RF and Microw. Computer-Aided Engg.*, Vol. 31, No. 11, 1–13, Nov. 2021.
10. Ansys High Frequency Structural Simulator, (HFSS), Version 16.2.
11. Kumar, G. and K. P. Ray, *Broadband Microstrip Antennas*, Artech House, Boston, London, 2002.
12. Mishra, M., S. Chaudhuri, R. S. Kshetrimayum, A. Alphones, and K. P. Esselle, "Space efficient meta-grid lines for mutual coupling reduction in two-port planar monopole and DRA array," *IEEE Access*, Vol. 10, 49829–49838, Jan. 2022.